Quasiparticle current in ballistic constrictions with finite transparencies of interfaces

B. A. Aminov
Department of Physics, University of Wuppertal, 42097 Wuppertal, Germany

A. A. Golubov* and M. Yu. Kupriyanov†
Institute of Thin Film and Ion Technology, Research Centre, Kernforschungsanlage Jülich G.m.b.H., D-52425 Jülich, Germany
(Received 1 August 1995)

Nonstationary properties of ballistic constrictions $SN/c/NS$ with disordered NS electrodes are analyzed theoretically. Amplitudes of Andreev and normal reflections at the constriction are related to the solutions of a stationary Green's function problem in an inhomogeneous NS electrode in the dirty limit. This provides a generalization of the model of Octavio, Tinhkam, Blonder, and Klapwijk for a spatially inhomogeneous case. The relation between the quasiparticle current in $SN/c/NS$ junctions and the energy spectrum of a NS proximity sandwich is found for arbitrary parameters of N and S materials and of NS interfaces. The effect of the proximity layer on the excess current and the subharmonic structure are analyzed in detail and related to the parameters of the S and N materials. The appearance of series of subharmonic peaks associated with the two-gap structure in the density of states of NS electrodes is demonstrated.

I. INTRODUCTION

Tunnel junctions with high critical current density are presently a subject of extensive experimental investigation (see Ref. 1 and references therein). As was shown in Ref. 1, barriers in Nb-AlO_x-Nb junctions with high J_c are likely to be a series of constrictions each having rather high transparency, and therefore they do not fulfill conditions of a standard tunnel theory. Additionally, a proximity layer near the barrier consisting either of a normal metal N or of a superconductor S' with reduced critical temperature T_c' is usually present in Nb-AlO_x-Nb or NbN/Nb-AlO_x-Nb/NbN junctions. The existence of such proximity layers is a consequence of the Nb technology,[2] where the dielectric barrier of a junction is produced by the deposition of a thin layer of another material onto the lower electrode. In most cases a thin Al overlayer on the Nb base electrode is used, which is subsequently oxidized and often covered with a second thin Al layer. As a result, some residual Al layers appear adjacent to the dielectric barrier, and the tunnel structure is Nb/Al/AlO_x/Al/Nb. Similar structures are created in the case of NbN junctions.[3] Moreover, in junctions used for some practical applications like particle or phonon detectors such residual layers are specially produced and used advantageously for collecting excess quasiparticles near the tunnel barrier.[4] Thus the resulting junctions are of $SNINS$ type, where N denotes a normal metal or a superconductor with smaller T_c in comparison with that of a superconductor S.

In low J_c junctions the transparency of a tunnel barrier is sufficiently small and the conditions of a standard tunnel theory[5,6] are fulfilled. In the regime of tunneling transport through a structureless barrier the properties of $SNINS$ junctions have been discussed theoretically in a number of papers.[7–16] The above approaches differ in the way of calculation of the densities of states in NS electrodes of a junction, but the tunneling regime is essentially used in all of them. However, for high J_c junctions another model, namely a small ballistic $SN/c/NS$ constriction (here c is the constriction and slash denotes the barrier), is a suitable starting point to discuss more complicated models. In this case the standard tunnel theory is not applicable, and the transport through a constriction with finite transparency should be considered instead of the tunneling through the barrier I.

The properties of $S/c/S$ constrictions with spatially homogeneous and equilibrium superconducting electrodes are presently well understood. The widely used model is based on the theory of Andreev and normal reflection processes at the NS interface developed by Blonder, Tinkham, and Klapwijk[17] (BTK model). This theory was applied to $S/c/S$ junctions by Klapwijk *et al.*, and Octavio *et al.*[18,19] (KBT and OTBK models). In their approach, the current through a constriction is fully determined by the amplitudes of normal and Andreev reflections at two S/c interfaces. Andreev reflection processes lead to the existence of excess current at large voltages, whereas the subharmonic gap structure (SGS) on I-V curves is naturally explained to be due to multiple Andreev reflections (MAR) at the constriction. Later, a microscopic theory of current transport through a $S/c/S$ constriction was developed by Zaitsev[20] and Arnold[21] with the Green's functions approach and applied to calculation of the SGS in $S/c/S$ contacts.[21] We note that the phenomenological OTBK approach does not take into account inelastic relaxation in the constriction region as well as interference between two S/c boundaries due to superconducting phase difference and resonant tunneling. However, as it was shown explicitly in Ref. 19, both the OTBK approach and the microscopic theory[21] predict the same positions of the SGS peaks $eV_n = 2\Delta/n$ in a phase-independent quasiparticle current component. Therefore the OTBK model can serve as a basis for calculation of the quasiparticle current in a more complex $SN/c/NS$ junction.

Whereas the condition of thermal equilibrium is generally fulfilled for the constriction geometry, the other condition of spatial homogeneity of the superconducting electrodes is less general. An important case of an inhomogeneous system is the above mentioned $SN/c/NS$ constriction. Previously, only

properties of clean $N/c/N'S$ contacts with small transparency of the $N'S$ interface were considered in Refs. 21,22. Thus the existing theoretical models do not cover the practically interesting case of $SN/c/NS$ proximity effect junctions with disordered electrodes (dirty limit), of arbitrary parameters of S and N materials, and the SN interface.

The purpose of the present work is to calculate the quasiparticle current of such junctions. The physical model of the $SN/c/NS$ structure assumes two disordered SN electrodes connected by a small ballistic constriction of the size smaller than the mean free path in SN. In this case the potential drop takes place at the constriction, and therefore the electrodes are in thermal equilibrium. The ballistic condition is important. It should be compared with the opposite limit of a disordered constriction of a size larger than the mean free path. The latter case was studied theoretically by Artemenko, Volkov, and Zaitsev[23] for $S/c/S$ constrictions.

Our approach to $SN/c/NS$ junctions is based on our previous work on $N/c/N'S$ constrictions.[24] The model of Ref. 24 is closely related to the original BTK one, generalizing the BTK model for the case of spatial inhomogeneous electrodes. The microscopic Green's functions approach was used to express coefficients of Andreev and ordinary electron reflections at the ballistic constriction via the energy spectrum of the disordered SN system. As a result the quasiparticle current for the $N/c/N'S$ contact was calculated microscopically, retaining the simplicity and direct physical meaning of the BTK model. In this paper we demonstrate the relation between properties of SN electrodes and the structure on I-V curves of $SN/c/NS$ junctions. In particular, the positions of subharmonic peaks will be discussed. Apart from the fundamental interest, the results of these calculations can be used for the interpretation of various experimental data, including high J_c Josephson tunnel junctions, high T_c SNS junctions, and tunneling spectroscopy of proximity multilayered systems.[25,22]

II. THE MODEL

Let us consider the boundary between the left SN and the right NS electrodes as a small constriction of size $a \ll \min(l_s, l_n)$, where l_s, l_n are the mean free paths of S and N. We assume that the N and S metals are in the dirty limit $l_{n,s} \ll \xi_{n,s}$.

The theoretical description of $S/c/S$ contacts was elaborated by Octavio, Tinkham, Blonder, and Klapwijk (OTBK).[18] They modeled a point contact as a superconductor–constriction-superconductor structure with elastic scattering at S/c interfaces, which can be simulated by a δ-function potential of strength H: $V(x) = H \times \delta(x)$ [or, in reduced units, $Z = H/(\hbar v_F)$ with the Fermi velocity v_F]. The Z factor is related to the normal transmission coefficient D by $(1+2Z^2) = D^{-1}$. Inelastic relaxation in the constriction region and interference of two S/c interfaces are neglected in the model.

Following the OTBK model, the quasiparticle current across a $S/c/S$ contact can be calculated for a one-dimensional geometry as

$$I = \frac{1}{eR_0} \int_{-\infty}^{\infty} [f_{\rightarrow}(\epsilon) - f_{\leftarrow}(\epsilon)] d\epsilon, \tag{1}$$

where $R_0 = [2N_1(0) A e^2 v_{F1}]^{-1}$ is the Sharvin resistance,[26] A is the contact area, $N_1(0)$ and v_{F1} are the density of states per spin, and the Fermi velocity of the constriction material, respectively. The functions $f_{\rightarrow}(E)$ and $f_{\leftarrow}(E)$ denote nonequilibrium distribution functions of right- and left-going charges. They are simply related by

$$f_{\rightarrow}(\epsilon) = 1 - f_{\leftarrow}(-\epsilon - eV). \tag{2}$$

The distribution function $f_{\rightarrow}(\epsilon)$ can be found self-consistently:[18]

$$f_{\rightarrow}(\epsilon) = A(\epsilon) f_{\rightarrow}(\epsilon - eV) + B(\epsilon)[1 - f_{\rightarrow}(-\epsilon - eV)] + T(\epsilon) f_0(\epsilon). \tag{3}$$

The coefficients $A(\epsilon)$, $B(\epsilon)$, and $T(\epsilon)$ denote the probabilities for Andreev scattering, elastic scattering, and transmission, and $f_0(\epsilon)$ is the Fermi-Dirac distribution function. Provided the energy dependencies $A(\epsilon)$, $B(\epsilon)$, and $T(\epsilon)$ are known, the $f_{\rightarrow}(\epsilon)$ function can be found numerically by an iterative procedure.

Only two of the coefficients $A(\epsilon)$, $B(\epsilon)$, and $T(\epsilon)$ need to be determined, since the conservation of probability requires that

$$A(\epsilon) + B(\epsilon) + T(\epsilon) = 1. \tag{4}$$

The OTBK model was shown to be at least in qualitative agreement with the results of microscopic calculations of Arnold.[19]

The processes of Andreev and normal reflection of a quasiparticle incident from a normal region into a disordered NS sandwich were analyzed theoretically in Ref. 24. It was shown that the solution of Gor'kov equations[27] in the N region at distances from the constriction smaller than l_n has the form of plane waves:

$$\begin{pmatrix} G_\epsilon(x,x') \\ F_\epsilon(x,x') \end{pmatrix} = C(x') \begin{pmatrix} g(x) \\ f(x) \end{pmatrix} e^{iq_2^+ x} + D(x') \begin{pmatrix} f(x) \\ g(x) \end{pmatrix} e^{-iq_2^- x}, \tag{5}$$

where $g(x)$ and $f(x)$ are quasiclassical Green's functions which determine the amplitudes for the excitation to be respectively into the electronlike or into the holelike states. In the dirty limit the relation between f, g and averaged over the Fermi surface functions $\langle F_\epsilon \rangle, \langle G_\epsilon \rangle$ is

$$\frac{f(x)}{g(x)} = \frac{i\langle F_\epsilon(x) \rangle}{1 + \langle G_\epsilon(x) \rangle}. \tag{6}$$

The functions $\langle F_\epsilon(x) \rangle$, $\langle G_\epsilon(x) \rangle$ obey diffusionlike equations[28,29] with the boundary conditions derived in Ref. 30.

On the other hand, one can write down the solution of the Bogolubov–de Gennes equations for the wave transmitted into the SN region:

$$\psi_{\text{trans}} = c \begin{pmatrix} u_0 \\ v_0 \end{pmatrix} e^{iq_2^+ x} + b \begin{pmatrix} v_0 \\ u_0 \end{pmatrix} e^{-iq_2^- x},$$

$$\hbar q_{1,2}^{\pm} = \sqrt{2m_{1,2}(\mu \pm \epsilon)}, \tag{7}$$

where m and ϵ are respectively the quasiparticle effective mass and energy, whereas u_0, v_0 are respectively the amplitudes of electronlike and holelike excitations. Matching the solutions (5), (7), and using the relation (6) together with the normalization condition $\langle G_\epsilon^2\rangle+\langle F_\epsilon^2\rangle=1$ one finally obtains the expressions for the Andreev reflection $A(\epsilon)$, the normal reflection $B(\epsilon)$, and the transmission $T(\epsilon)$ coefficients:[24]

$$A(\epsilon)=\frac{|\langle F_\epsilon(0+)\rangle|^2}{|1+2Z^2+\langle G_\epsilon(0+)\rangle|^2}, \tag{8}$$

$$B(\epsilon)=\frac{4Z^2(1+Z^2)}{|1+2Z^2+\langle G_\epsilon(0+)\rangle|^2}, \tag{9}$$

$$T(\epsilon)=\frac{2(1+2Z^2)\mathrm{Re}\langle G_\epsilon(0+)\rangle}{|1+2Z^2+\langle G_\epsilon(0+)\rangle|^2}. \tag{10}$$

The relations (8)–(10) show that in the dirty limit the coefficients $A(\epsilon), B(\epsilon)$, and $T(\epsilon)$ are directly related to the local energy spectrum in N near the constriction. In particular, the local density of states near the constriction is given in the usual way as $N(\epsilon)=\mathrm{Re}\{\langle G_\epsilon(0+)\rangle\}$ which demonstrates explicitly the relation between the transmission coefficient (10) and $N(\epsilon)$. The expressions (8)–(10) generalize the corresponding BTK relations[17] for a spatially inhomogeneous case. In a spatially homogeneous case Green's functions are given by $\langle G_\epsilon(0+)\rangle=-i\epsilon/\sqrt{\Delta_0^2-\epsilon^2}$, $\langle F_\epsilon(0+)\rangle=\Delta_0/\sqrt{\Delta_0^2-\epsilon^2}$, and the BTK relations follow from Eqs. (8) and (9).

Thus, according to Eqs. (1), (3), and (8)–(10), the current implicitly depends on the Green's functions $\langle G_\epsilon(0+)\rangle$ and $\langle F_\epsilon(0+)\rangle$ and the problem is reduced to the solution for the proximity effect in the dirty SN sandwich. The proximity effect in dirty NS sandwiches was studied previously in Refs. 30, 16 for the case of arbitrary transparency of the N/S interface. The angle averaged quasiclassical Green functions $G(\epsilon,x)=\cos\theta(\epsilon,x)$, $F(\epsilon,x)=\sin\theta(\epsilon,x)$ in the dirty NS bilayer satisfy the equation

$$\xi_{N,S}^2\theta''_{N,S}(x)+i\epsilon\,\sin\theta_{N,S}(x)+\Delta_{N,S}(x)\cos\theta_{N,S}(x)=0, \tag{11}$$

where $\xi_{N,S}$, $\Delta_{s',s}$ is the order parameter. To be more specific, we shall discuss below the particular case of $\Delta_n=0$, i.e., of $T_{c'}=0$ (NS sandwich). The generalization to the case of nonzero $T_{c'}$ is straightforward[15,16] and can be mainly taken into account by proper renormalization of the proximity effect parameters, which does not change our results qualitatively.

The boundary conditions at the NS interface ($x=0$) have the form[30]

$$\gamma_B\xi_N\theta'_N=\sin(\theta_S-\theta_N),$$
$$\gamma\xi_N\theta'_N=\xi_s\theta'_S, \tag{12}$$

whereas in the bulk of the S layer

$$\theta_s(\infty)=\arctan[i\Delta_0(T)/\epsilon] \tag{13}$$

and at the N metal free surface ($x=-d_N$)

$$\theta'_N(-d_N)=0. \tag{14}$$

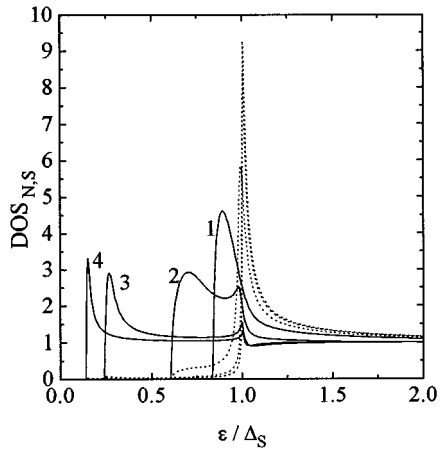

FIG. 1. Density of states in the N layer of a NS sandwich normalized to their normal-state values at the free surface (solid lines) and at the NS boundary (dashed lines) for $\gamma_m=0.1$ and different $\gamma_B=0$ (curve 1), $\gamma_B=1$ (2), $\gamma_B=5$ (3), and $\gamma_B=10$ (4).

The self-consistency equation for the order parameter in the S region has the form

$$\Delta_s(x)\ln\frac{T}{T_c}+2\frac{T}{T_c}\sum_{w_n}\left[\frac{\Delta_s(x)}{\omega_n}-\sin\theta_s(x,\epsilon=i\omega_n)\right]=0. \tag{15}$$

The parameters γ_B and γ

$$\gamma_{BN}=\frac{R_B}{\rho_N\xi_N},\quad \gamma=\frac{\rho_S\xi_S}{\rho_N\xi_N} \tag{16}$$

have simple physical meanings: γ is a measure of the strength of the proximity effect between the S and N metals, whereas γ_{BN} describes the effect of the boundary transparency between these layers. Here $\rho_{N,S}$, $\xi_{N,S}=\sqrt{D_{N,S}/2\pi T_c}$ and $D_{N,S}$ are normal state resistivities, coherence lengths, and diffusion constants of the N and S metals, respectively, while R_B is the product of the resistance of the NS boundary and its area. We have normalized ϵ and $\Delta(x)$ to πT_c, where T_c is the critical temperature of the bulk S. To reduce the number of parameters, only the case of a thin N layer, $d_N/\xi_N\ll 1$, will be discussed below. Then the parameters of the proximity effect problem are $\gamma_m=\alpha\gamma d_N/\xi_N$ and $\gamma_B=\alpha\gamma_{BN}d_N/\xi_N$. Here $\alpha=\ln(T_c/T_{c'})/\ln(2\gamma^*\Omega_d/\pi T_{c'})$, where $T_{c'}$ is the critical temperature of the N layer,[30,16] $\Omega_d=\pi T_c(\xi_N/d_N)^2$, and $\gamma^*\simeq 1.78$ is the Euler's constant. The dependence of the parameter α on $T_{c'}/T_c$ can be found in Ref. 16.

For the case of arbitrary values of the parameters γ and γ_B the boundary value problem (11)–(16) was solved numerically. Using the solutions $\theta_N(\epsilon,x)$, one can calculate the local density of states $N(\epsilon,x)=\mathrm{Re}\cos\theta_N(\epsilon,x)$ at any point of the system. Some typical results of the calculations of the densities of states $N(\epsilon)$ at low temperatures $T=0$ in the N region near the constriction (solid lines) and in the S region near the NS boundary (dotted lines) are presented in Figs. 1 and 2 [here and below Δ_s denotes the bulk gap $\Delta_0(T)$].

It is seen that at small γ_m values two peaks exist in $N(\epsilon)$ in the N region. The first peak corresponds to the energy gap in N, Δ_N, which is reduced in comparison to the

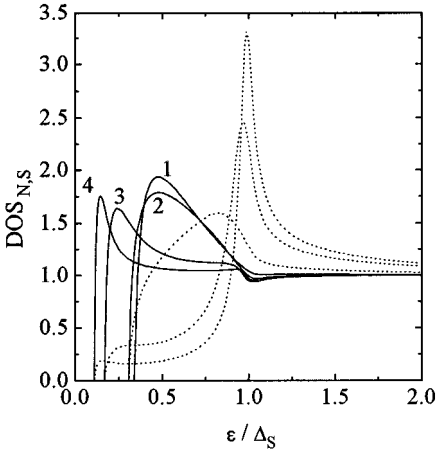

FIG. 2. Density of states in the N layer of a NS sandwich normalized to their normal-state values at the free surface (solid lines) and at the NS boundary (dashed lines) for $\gamma_m=1$ and different $\gamma_B=0$ (curve 1), $\gamma_B=1$ (2), $\gamma_B=5$ (3), and $\gamma_B=10$ (4).

bulk gap Δ_s, whereas the second peak corresponds to Δ_S. As will be shown below, this two-gap structure manifests itself on I-V curves of the $SN/c/NS$ constriction. It is also seen from comparison of Figs. 1 and 2, the second peak at $\epsilon=\Delta_S$ is smeared out with the increase of the parameter γ_m, whereas an increase of γ_B (decrease of the NS boundary transparency) leads to the reduction of the smaller gap Δ_N which scales as $\sim\Delta_S/\gamma_B$ for large $\gamma_B\gg 1$.

Using the above results, one can calculate the coefficients $A(\epsilon)$, $B(\epsilon)$, and $T(\epsilon)$ which are related to the values of $G(\epsilon,x)=\cos\theta(\epsilon,x)$ and $F(\epsilon,x)=\sin\theta(\epsilon,x)$ in the dirty SN bilayer near the constriction (at $x=-d_N$). The results of calculations are shown in Figs. 3 and 4 for a representative set of parameters. For subgap energies $\epsilon<\Delta_N$ the transmission coefficient $T(\epsilon)=0$, which corresponds to the fact that Δ_N is the real proximity-induced energy gap in the quasiparticle spectrum in the N region. At finite γ_B values an additional structure in the coefficients $A(\epsilon)$, $B(\epsilon)$, and $T(\epsilon)$ is present. The peak at $\epsilon=\Delta_S$ in $N(\epsilon)$ appears as a sharp singularity in the reflection and transmission probabilities (Figs. 3 and 4).

III. THE RESULTS

With coefficients $A(\epsilon)$, $B(\epsilon)$, and $T(\epsilon)$ determined from the solution of the proximity effect problem, a calculation of the quasiparticle current can be done according to the OTBK method (1),(3). First, the distribution functions $f_{\rightarrow}(\epsilon)$ and $f_{\leftarrow}(\epsilon)$ are calculated iteratively. Figures 5 and 6 demonstrate the typical structure of solutions for $f_{\rightarrow}(\epsilon)$ for $T=0$ K and bias voltage $eV=2\Delta_S$. The structure in $f_{\rightarrow}(\epsilon)$ is rather simple for the case $Z=0$, reflecting two energy gaps in the N region, whereas for $Z\neq 0$ a more complicated structure appears due to multiple Andreev and normal reflections within the constriction. We will return to the interpretation of this structure later.

Using the solutions for $f_{\rightarrow}(\epsilon)$ and $f_{\leftarrow}(\epsilon)$, one straightforwardly calculates the I-V curves according to Eq. (1). The results of calculations for representative parameters sets are presented in Figs. 7, 9–11.

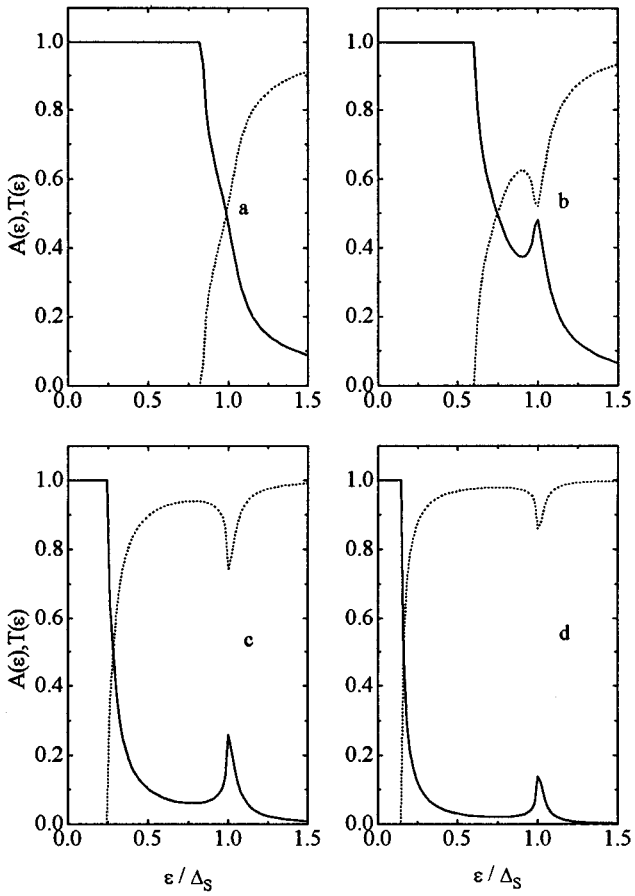

FIG. 3. Probabilities of Andreev reflection $A(\varepsilon)$ (solid lines) and of transmission $T(\varepsilon)$ (dotted lines) for the ballistic $SN/c/NS$ constriction for $Z=0$, $\gamma_m=0.1$ and different $\gamma_B=0$ (a), $\gamma_B=1$ (b), $\gamma_B=5$ (c), and $\gamma_B=10$ (d).

Let us start our discussion with the case when the normal scattering on the constriction boundary is absent ($Z=0$) and $T=0$ K. For a vanishing proximity layer $d_N\rightarrow 0$ the OTBK result for a $S/c/S$ constriction was reproduced [curve 1, Figs. 7(a,b)]. For this case a large excess of current of $I_{\rm ex}=I(V\gg\Delta/e)-V/R_N=8/3(\Delta/eR_N)$ without any visible structure can be seen on the current-voltage characteristic [curve 1, Fig. 7(a)]. The absence of the subharmonic structure in this case is related to the fact that all quasiparticles from the condensate participate in the current transfer. Indeed, each of them is able finally to overcome the energy gap, because there is no limitation for the number of Andreev reflections for $Z=0$. The introducing of the proximity layer results in the decreasing of the excess current and in the appearance of the subharmonic structure [curves 2–4, Figs. 7(a,b)]. The structure reveals as peaks (maxima) in the dynamic conductivity at voltages $V_n=(\Delta_S-\Delta_N)/(en)$. The amplitude of subharmonic peaks depends on the SN-boundary transparency (γ_B parameter).

To understand the origin of this structure, we return to Fig. 1 of the density of states $N(\epsilon)$ in the N region. As it was mentioned above, for small γ_m parameters $N(\epsilon)$ has two peaks at energies $\epsilon=\Delta_S$ and Δ_N related to the volume and proximity induced energy gaps (Fig. 1). The peak at $\epsilon=\Delta_S$

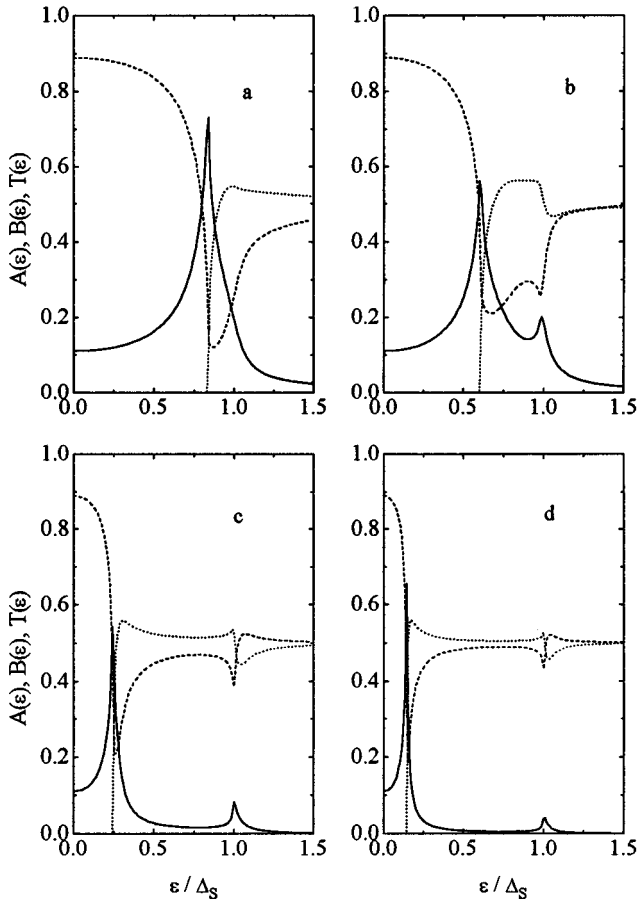

FIG. 4. Probabilities of Andreev reflection $A(\varepsilon)$ (solid lines), of normal reflection $B(\varepsilon)$ (short dashed lines) and of transmission $T(\varepsilon)$ (dotted lines) for the ballistic $SN/c/NS$ constriction for $Z=1$, $\gamma_m=0.1$ and different $\gamma_B=0$ (a), $\gamma_B=1$ (b), $\gamma_B=5$ (c), and $\gamma_B=10$ (d).

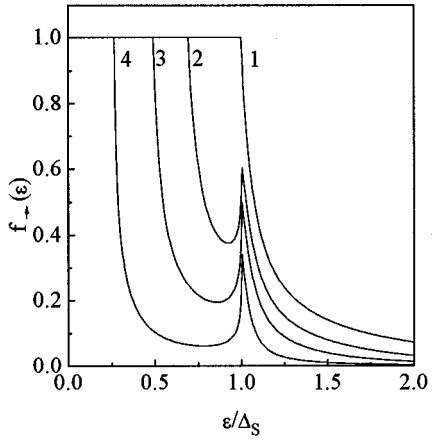

FIG. 5. Zero-temperature distribution functions $f_{\rightarrow}(\varepsilon)$ for the ballistic $SN/c/NS$ constriction at voltage bias $eV=2\Delta_S$, $Z=0$, $\gamma_m=0.01$, and different $\gamma_B=1$ (curve 2), $\gamma_B=2$ (3), and $\gamma_B=5$ (4). For comparison the $f_{\rightarrow}(\varepsilon)$ for an $S/c/S$ constriction ($\gamma_{m,B}=0$) is shown (curve 1).

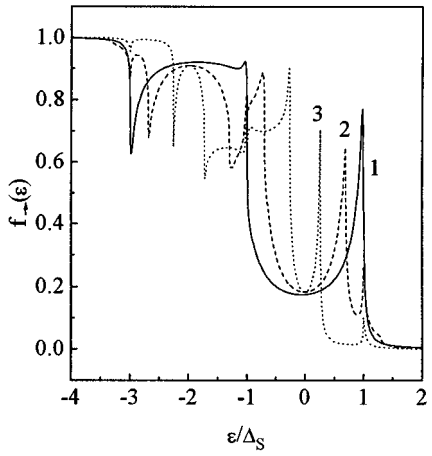

FIG. 6. Zero-temperature distribution functions $f_{\rightarrow}(\varepsilon)$ for the ballistic $SN/c/NS$ constriction at voltage bias $eV=2\Delta_S$, $Z=1$, $\gamma_m=0.01$ and different $\gamma_B=1$ (curve 2) and $\gamma_B=5$ (curve 3). For comparison the $f_{\rightarrow}(\varepsilon)$ for $S/c/S$ constriction ($\gamma_{m,B}=0$) is shown (curve 1).

in $N(\epsilon)$ appears as a sharp singularity in the Andreev reflection probability (Fig. 3) and in the distribution function $f_{\rightarrow}(\varepsilon)$ (Fig. 5). Thus the proximity effect plays here the same role as a temperature for $Z=0$ or a normal reflection from the S/c boundary for $Z\neq 0$ in $S/c/S$ constrictions, but

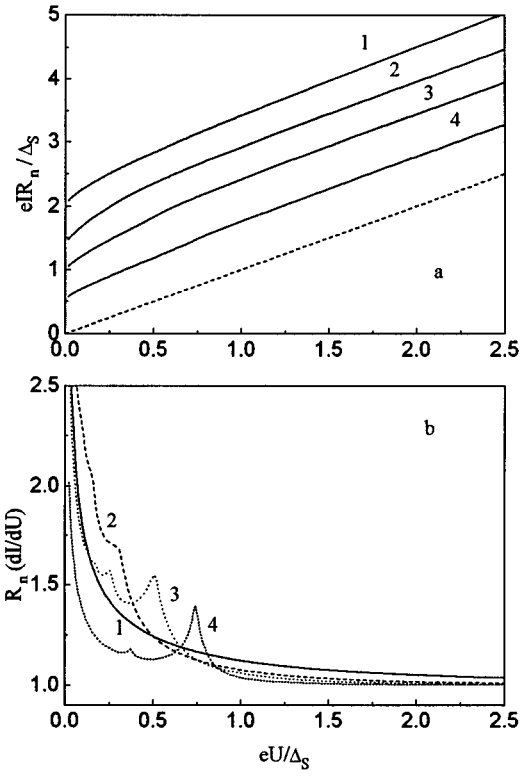

FIG. 7. Normalized current-voltage (a) and differential conductance-voltage (b) characteristics for a $SN/c/NS$ constriction in the absence of scattering on the N/c boundary ($Z=0$) at $T=0$ K for $\gamma_m=0.01$ and different $\gamma_B=1$ (curves 2), $\gamma_B=2$ (3), and $\gamma_B=5$ (4). The characteristics for an $S/c/S$ constriction ($\gamma_{m,B}=0$) are shown for comparison (curves 1).

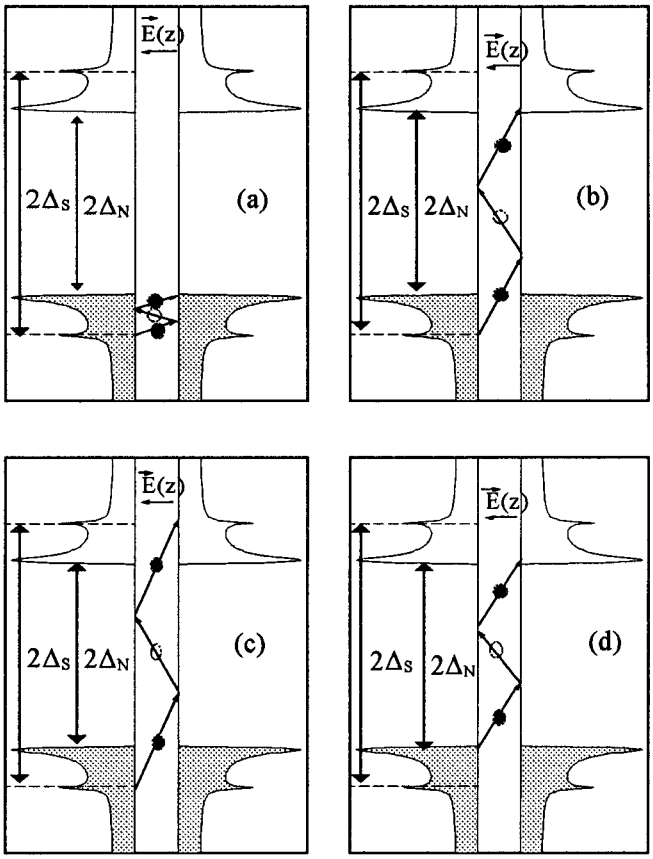

FIG. 8. Schematic representation of quasiparticle trajectories in the constriction region suffering multiple Andreev reflection at $T=0$ K and at bias voltages: (a) $eV=(\Delta_S-\Delta_N)/3$; (b) $eV=(\Delta_S+\Delta_N)/3$; (c) $eV=2\Delta_N/3$; (d) $eV=2\Delta_S/3$.

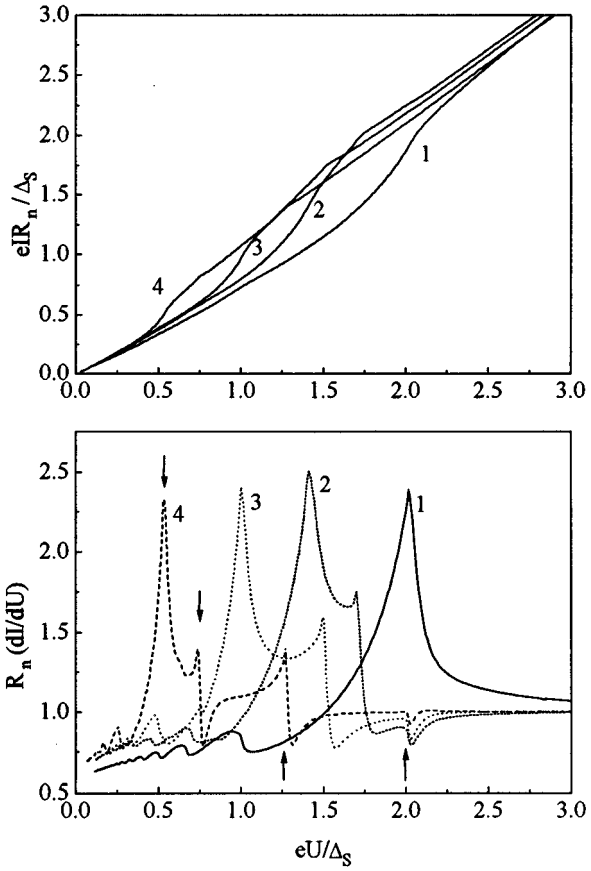

FIG. 9. Normalized current-voltage (a) and differential conductance-voltage (b) characteristics for a $SN/c/NS$ constriction for $Z=1$ at $T=0$ K, for $\gamma_m=0.01$ and different $\gamma_B=1$ (curves 2), $\gamma_B=2$ (3), and $\gamma_B=5$ (4). The characteristics for an $S/c/S$ constriction ($\gamma_{m,B}=0$) are shown for comparison (curves 1). By arrows the first SGS peak is indicated of the $V_n=2\Delta_N/(en)$, $V_n=(\Delta_S-\Delta_N)/(en)$, $V_n=(\Delta_S+\Delta_N)/(en)$, and $V_n=2\Delta_S/(en)$ series (from left to right).

with one essential difference. The temperature-activated or normally reflected quasiparticles give a negative contribution to the current. This produces negative peaks (minima) in the dynamic conductance.[18,31] Whereas, in $SN/c/NS$ constrictions a multiple Andreev reflection process with $V_n=(\Delta_S-\Delta_N)/(en)$ subharmonics contributes an additional current in the same direction and produces positive peaks in the dynamic conductance. Schematically, this process with two Andreev reflections is shown in Fig. 8(a). An electron from the left electrode with an energy close to the volume superconducting energy gap Δ_S is accelerated by the applied electric field $\vec{E(z)}$, suffers two Andreev reflections on N/c boundaries and finally remains in the right electrode at energies close to Δ_N. Such a process is possible due to a finite probability of Andreev reflections in the $(\Delta_S-\Delta_N)$ energy range, as is shown in Fig. 3, and is specific for the considered $SN/c/NS$ junctions. Passing through the constriction range quasiparticles gain the energy eV. For the process with n multiple Andreev reflections the total energy gain reaches $(n+1)$ eV.

The I-V characteristics of contacts with a finite potential barrier on the N/c boundary ($Z\neq 0$) show an essentially more reach structure, as can be seen from Fig. 9. In contrast to spatially homogeneous $S/c/S$ constrictions with $Z\neq 0$,

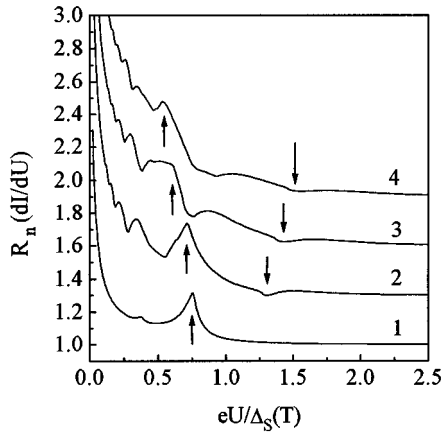

FIG. 10. Normalized differential conductance vs the voltage for a $SN/c/NS$ constriction for $Z=0$, $\gamma_m=0.1$, $\gamma_B=5$ and at different temperatures: curve $1-T/T_c=0$; $2-T/T_c=0.7$; $3-T/T_c=0.9$; $4-T/T_c=0.95$. By the upward and downward arrows $eV=\Delta_S-\Delta_N$ and $eV=\Delta_S+\Delta_N$ peaks are indicated.

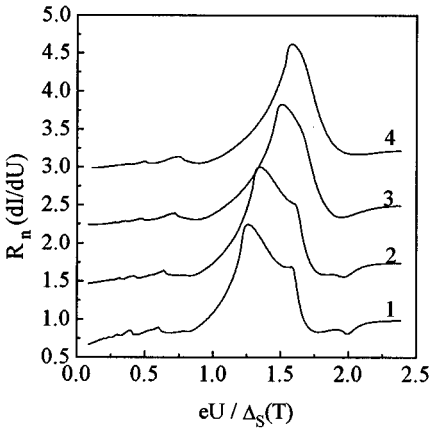

FIG. 11. Normalized differential conductance vs the voltage normalized to the temperature dependent volume energy gap $\Delta_S(T)$ for a $SN/c/NS$ constriction for $Z=1$, $\gamma_m=0.1$, $\gamma_B=5$ and at different temperatures: curve $1-T/T_c=0$; $2-T/T_c=0.7$; $3-T/T_c=0.9$; $4-T/T_c=0.95$.

where $A(\epsilon)$ has a one-peak structure at $\epsilon=\Delta_S$, $A(\epsilon)$ for $SN/c/NS$ constrictions reveals two peaks at $\epsilon=\Delta_S$ and Δ_N. This causes a strong modification of the $f_{\rightarrow}(\epsilon)$ and $f_{\leftarrow}(\epsilon)$ distribution functions (Fig. 6). For a $S/c/S$ constriction $f_{\rightarrow}(\varepsilon)$ is defined as a sharply-peaked curve with an $eV=2\Delta_S$ periodical structure (for $V=2\Delta_S/e$ applied bias voltage). This periodical structure is responsible for the first $(n=1)$ subharmonic peak of the $V_n=2\Delta_S/(en)$ series. The proximity layer results in a splitting of the peaked structure and decrease the amplitude of the old peaks (Fig. 6). Remarkable, that even for large γ_B parameters the $V_n=2\Delta_S/(en)$ SGS series is still present. A two-gap density of states opens three additional MAR processes with new SGS series: $2\Delta_N/n$, $(\Delta_S-\Delta_N)/n$, and $(\Delta_S+\Delta_N)/n$. Schematically, these processes are shown in Figs. 8(a,b,d).

The first SGS peak in the differential conductivity for all four series is indicated by arrows on Fig. 9(b) for the case of $\gamma_B=5$. The higher-order harmonics [except for the $V_n=2\Delta_N/(en)$ series] have essentially smaller amplitudes, which complicates their identification. The second-derivatives $d^2I(V)/dV^2$ are more informative in this case where SGS manifests itself as a series of negative peaks.

Note that the normal reflection adds a negative contribution to the current. In this case the SGS corresponds to the minima in the differential conductance. Only for the $V_n=(\Delta_S-\Delta_N)/(en)$ MAR process a combination of the positive and negative contributions takes place.

As it was shown by KBT,[18] the effect of the temperature on $S/c/S$ constrictions with $Z=0$ is similar to the normal scattering at the NS boundary at $T=0$ K. For finite temperatures the generation of a SGS is associated with the negative contribution to the current from thermally-activated quasiparticles.[31] For $SN/c/NS$ constrictions the situation differs in respect to the presence of the $V_n=(\Delta_S-\Delta_N)/(en)$ SGS series even at $T=0$ K (Fig. 7). For nonzero temperatures two SGS series appear $V_n=2\Delta_N/(en)$ and $V_n=(\Delta_S+\Delta_N)/(en)$ (Fig. 10). Note the absence of the $V_n=2\Delta_S/(en)$ SGS series. Thus an increase of temperature and a normal reflection in $SN/c/NS$ constrictions manifest themselves on I-V curves in a different way.

With increasing temperature the difference between Δ_N and Δ_S decreases, which can be interpreted as an enhancement of the proximity effect. The $V=(\Delta_S-\Delta_N)/e$ peak shifts to lower voltages, whereas $(\Delta_S+\Delta_N)/e$ moves to higher voltages, as is indicated in Fig. 10. The same effect is present for $SN/c/NS$ constrictions with $Z=1$, where $V=2\Delta_N/e$ and $V=(\Delta_S+\Delta_N)/e$ peaks merge with increasing temperature (Fig. 11).

This enhancement of the proximity effect can be explained in the present model in the following way. As follows from the equations of the proximity effect model discussed above, for a small γ_m/γ_B ratio one can in the first approximation neglect spatial gradients in S and assume for the order parameter $\Delta_S(x)$ the BCS value $\Delta_0(T)$. Then the solution of Eq. (11) with boundary condition, (12),(14) yields the equation for the energy gap Δ_{gN} in the N layer:

$$\Delta_{gN}(T)=\frac{\Delta_0(T)}{1+\gamma_B\sqrt{\Delta_0^2(T)-\Delta_{gN}^2(T)}/\pi T_c}. \qquad (17)$$

For large γ_B (small transparency of the NS interface) the gap Δ_{gN} is small and at low temperatures $\Delta_0(T)\gamma_B/\pi T_c \gg 1$ is given by $\Delta_{gN}(T)\simeq \pi T_c/\gamma_B \ll \Delta_0(T)$. This relation is not fulfilled at temperatures near T_c when $\Delta_0(T)$ becomes small. In the latter case, when $\Delta_0(T)\gamma_B/\pi T_c \ll 1$, Eq. (17) yields the result $\Delta_{gN}(T)=\Delta_0(T)$. Therefore both gaps Δ_{gN} and Δ_0 merge as the temperature is increased. This effect is also known from the McMillan proximity effect model valid for small transparency of the NS interface. As was shown in Ref. 16, the McMillan model can be derived from the above equations for the case of $\gamma_m/\gamma_B \ll 1$. The McMillan parameter is given by the relation $\Gamma_N=\pi T_c/\gamma_B$ and has the physical meaning of a coupling strength between N and S layers. Then, in the language of the McMillan model, a small gap $\Delta_{gN}(T)\simeq\Gamma_N$ is induced in N for small Γ_N at zero T, whereas with an increase of T the effective Γ_N parameter increases as $\Gamma_N(T)\sim\Gamma_N(0)\Delta(0)/\Delta(T)$. This

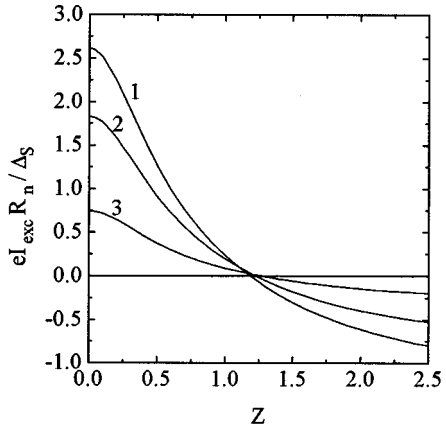

FIG. 12. Excess of current normalized to the volume energy gap Δ_S as a function of the scattering parameter Z at $T=0$ K for an $SN/c/NS$ constriction for $\gamma_m=0.1$ and different $\gamma_B=1$ (curve 2) and $\gamma_B=5$ (3). The result for a $S/c/S$ constriction ($\gamma_{m,B}=0$) is also presented (curve 1).

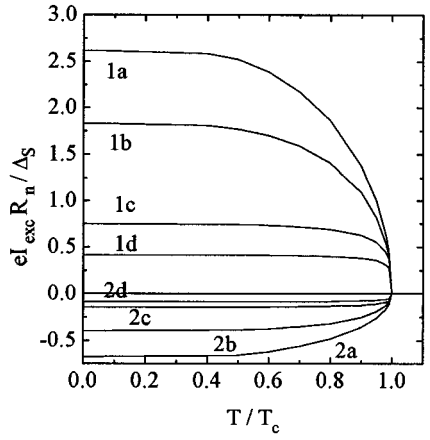

FIG. 13. Excess of current normalized to the zero-temperature volume energy gap Δ_S as a function of temperature for a $SN/c/NS$ constriction for (1) $Z=0$ and (2) $Z=2$. Calculations were performed for $\gamma_m=0.1$ and different $\gamma_B=1$ (curves b), $\gamma_B=5$ (c), and $\gamma_B=10$ (d). The result for a $S/c/S$ constriction ($\gamma_{m,B}=0$) is also presented (curves a).

fact means an increase of the coupling strength and, as a consequence, an enhancement of the proximity effect at higher T.

An excess current at large voltages $V \gg \Delta/e$ is another effect associated with Andreev reflection on a S/N boundary. The effect of the normal scattering Z on the excess current is illustrated in Fig. 12. For small Z the $I(V)$ curves exhibit a positive excess current. With increasing Z parameter the excess current changes the sign and becomes negative. The appearance of a proximity layer results in the decay of the transition from positive to negative $I_{\rm ex}$. Thus, for a small range of the Z parameter an increase of the positive excess current occurs by introducing the proximity layer. This effect is present on $I(V)$ curves in Fig. 9(a) for $Z=1$ and $\gamma_m=0.01$. The effect depends strongly both on the coupling strength between S and N layers (γ_m parameter) and on the SN-boundary transparency (γ_B parameter).

The temperature dependencies of the excess current are shown in Fig. 13 for $Z=0$, when the $I_{\rm ex}$ is positive, and for $Z=2$, when $I_{\rm ex}$ is negative. An increase of the γ_B parameter leads to the decrease of the absolute values of the excess current and to the deviation from $I_{\rm ex}(T)$ for the spatially homogeneous $S/c/S$ constriction, which is simply proportional to the BCS-temperature dependence of the energy gap. For large γ_B parameters $I_{\rm ex}(T)$ does not depend on temperature in the broad temperature range up to T_c, where the sharp drop of $I_{\rm ex}(T)$ takes place (Fig. 13). At temperatures close to T_c the magnitude of the excess current becomes essentially the same as for the $S/c/S$ constriction. This is another consequence of the enhancement of the proximity effect with increasing temperatures, as was discussed above.

IV. CONCLUSIONS

In conclusion, the OTBK model is generalized for a spatially inhomogeneous case of $SN/c/NS$ ballistic constrictions with disordered NS electrodes. The quasiparticle current is calculated for arbitrary parameters of N and S materials and their interface, if the conditions of the dirty limit are fulfilled. An energy gap in N is always present and its magnitude depends on the parameters of the S and N materials, as well as of the transparency of the SN interface. It is shown that the conductance of ballistic $SN/c/NS$ junctions reflects a proximity induced energy gap in N, and under certain conditions also the bulk gap of the superconductor S. The subharmonic structure and the excess current are analyzed in detail. It is shown that, in addition to the usual structure at $V_n=2\Delta_S/(ne)$, resonances at $V_n=(\Delta_S-\Delta_N)/(en)$, $V_n=2\Delta_N/(en)$, and $V_n=(\Delta_S+\Delta_N)/(en)$ are present in $SN/c/NS$ constrictions due to multiple Andreev reflection processes. For the case of a reflectionless constriction $Z=0$ the existence of a SGS at zero temperature at $V_n=(\Delta_S-\Delta_N)/(en)$ is demonstrated in contrast to the structureless $I(V)$ curves of $S/c/S$ constrictions.

ACKNOWLEDGMENTS

Stimulating discussions with D. Averin, A. Braginski, K. Likharev, and M. Siegel are gratefully acknowledged. The work was supported in part by the International Science Foundation under Grant No. MDP300, Russian Ministry of Scientific and Technical Policy in the frame of the Scientific Program ''Actual Problems of Condensed Matter Physics,'' and BMFT Germany under Grant No. 13N6329 and No. 13N6418.

* Permanent address: Institute of Solid State Physics, 14243 Chernogolovka, Russia.
† Permanent address: Nuclear Physics Institute, Moscow State University, 119899 Moscow, Russia.

[1] A.W. Kleinsasser, R.E. Miller, W.H. Mallison, and G.B. Arnold, Phys. Rev. Lett. **72**, 1738 (1994).
[2] M. Gurvitch, M.A. Washington, and H.A. Huggins, Appl. Phys. Lett. **42**, 472 (1983).
[3] J. Talvacchio, J.G. Gavaler, A.I. Braginski, and M.A. Janocko, J. Appl. Phys. **58**, 4638 (1985).
[4] N. Booth, Appl. Phys. Lett. **50**, 293 (1992).
[5] N.R. Werthamer, Phys. Rev. **147**, 255 (1966).
[6] A.I. Larkin and Yu.N. Ovchinnikov, Zh. Eksp. Teor. Fiz. **51**, 1535 (1966) [Sov. Phys. JETP **24**, 1035 (1967)].
[7] W.L. McMillan, Phys. Rev. **175**, 537 (1968).
[8] V.Z. Kresin, Phys. Rev. B **28**, 1294 (1983).
[9] G.B. Arnold, Phys. Rev. B **18**, 1076 (1978).
[10] A.D. Zaikin and G.F. Zharkov, Zh. Eksp. Teor. Fiz. **78**, 721 (1980) [Sov. Phys. JETP **51**, 364 (1980)]; **81**, 1781 (1981) [**54**, 944 (1981)].
[11] G. Kieselmann, Phys. Rev. B **35**, 6762 (1987).
[12] M. Ashida, S. Aoyama, J. Hara, and K. Nagai, Phys. Rev. B **40**, 8673 (1989).
[13] Y. Tanaka and M. Tsukada, Phys. Rev. B **47**, 287 (1993).
[14] A.A. Golubov and M.Yu. Kupriyanov, J. Low Temp. Phys. **70**, 83 (1988).
[15] A.A. Golubov, M.A. Gurwitch, M.Yu. Kupriyanov, and S.V. Polonskii, Sov. Phys. JETP **76**, 915 (1993).

[16] A.A. Golubov, E.P. Houwman, J.G. Gijsbertsen, V.M. Krasnov, J. Flokstra, and H. Rogalla, Phys. Rev. B **51**, 1073 (1995).
[17] G.E. Blonder, M. Tinkham, and T.M. Klapwijk, Phys. Rev. B **25**, 4515 (1982).
[18] T.M. Klapwijk, G.E. Blonder, and M. Tinkham, Physica (Amsterdam) **109-110B+C**, 1657 (1982); M. Octavio, M. Tinkham, G.E. Blonder, and T.M. Klapwijk, Phys. Rev. B **27**, 6739 (1983).
[19] K. Flensberg, J. Bindslee Hansen, and M. Octavio, Phys. Rev. B **38**, 8707 (1988).
[20] A.V. Zaitsev, Zh. Eksp. Teor. Fiz. **86**, 1742 (1984) [Sov. Phys. JETP **59**, 1015 (1984)].
[21] G.B. Arnold, J. Low Temp. Phys. **59**, 143 (1985); **68**, 1 (1987).
[22] A. Di Chiara, F. Fontana, G. Peluso, and F. Tafuri, Phys. Rev. B **48**, 6695 (1993).
[23] S.N. Artemenko, A.F. Volkov, and A.V. Zaitsev, Solid State Commun. **30**, 771 (1979).
[24] A.A. Golubov and M.Yu. Kupriyanov, JETP Lett. **61**, 851 (1995).
[25] D.R. Heslinga, S.E. Shafranjuk, H. van Kempen, and T.M. Klapwjik, Phys. Rev. B **49**, 10 484 (1994).
[26] Yu.V. Scharvin, JETP **21**, 655 (1965).
[27] A.A. Abrikosov, L.P. Gor'kov, and I.E. Dzyaloshinskii, *Methods of Quantum Field Theory in Statistical Physics* (Pergamon, New York, 1965).
[28] G.M. Eliashberg, Sov. Phys. JETP **34**, 668 (1971).
[29] A.I. Larkin and Yu.N. Ovchinnikov, Sov. Phys. JETP **41**, 960 (1975).
[30] M.Yu. Kupriyanov and V.F. Lukichev, Sov. Phys. JETP **67**, 1163 (1988).
[31] U. Gunsenheimer and A.D. Zaikin, Phys. Rev. B **50**, 6317 (1994).